Interaction of Hydrogen and Thiophene with Ni/MoS_2 and Zn/MoS_2 Surfaces: A Molecular Orbital Study

José A. Rodriguez

Department of Chemistry, Brookhaven National Laboratory, Upton, New York 11973

Received: April 11, 1997; In Final Form: June 15, 1997[⊗]

The effects of Ni and Zn on the electronic and chemical properties of MoS_2 clusters have been investigated using INDO/S and ab initio SCF calculations. The deposition of Ni or Zn atoms on a series of clusters (Mo_5S_{10}, Mo_6S_{12}, Mo_8S_{18}, Mo_9S_{18}, $Mo_{12}S_{24}$, and $Mo_{18}S_{36}$) that resemble the MoS_2(0002)-S and $MoS_2(10\bar{1}0)$-Mo surfaces produces a substantial reduction (0.5−2 eV) in the stability of the HOMOs of these systems. In all the cases examined, there was an admetal→MoS_2 charge transfer that increased the negative charge on S and reduced the positive charge on Mo. The electronic and chemical perturbations induced by Ni were much larger than those induced by Zn. Ab initio SCF results for Ni-promoted $MoS_2(10\bar{1}0)$-Mo clusters showed a simultaneous increase in the electron density on Mo and in the reactivity of this metal toward H_2 and thiophene. On the $(10\bar{1}0)$-Mo surface, Ni facilitated the dissociation of H_2 by largely increasing the stability of the transition state and products for this reaction. The bonding interactions between MoS_2(0002)-S clusters and H_2 or thiophene were weak. Ni and Zn adatoms enhanced the chemical activity of the (0002)-S surface by providing active sites for the dissociation of H_2 and the chemisorption of thiophene. The behavior of molybdenum sulfide catalysts in hydrogenation and hydrodesulfurization processes is discussed in light of these results.

I. Introduction

MoS_2 is the most widely used metal sulfide catalyst in the chemical and petroleum-refining industries.[1,2] Molybdenum sulfide is able to catalyze several chemical processes in which hydrogen is a reactant: synthesis of alcohols from CO,[3] the isomerization and hydrogenation of olefins,[4] and the hydrotreatment of oil-derived feedstocks (hydrodesulfurization, hydrodenitrogenation, and hydrodeoxygenation reactions).[5−8] By far the most important application of MoS_2 catalysts involves hydrodesulfurization (HDS) processes, where sulfur-containing molecules are removed from petroleum by reaction with hydrogen to form H_2S and hydrocarbons.[1,6−8] Organosulfur compounds are common impurities in crude oil that must be removed to avoid the poisoning of platinum-based catalysts in the refinement processes and the formation of SO_x pollutants when heavy oil is burned as fuel.[2] The industrial HDS catalysts are complex systems.[6−8] They frequently consist of a mixture of MoS_2 and Co or Ni on a γ-alumina support.[6−8] After comparing the effects of different metals (V, Cr, Fe, Co, Ni, Cu, and Zn) on the HDS activity of molybdenum sulfide catalysts, it was found that Co and Ni were strong promoters, while the rest of the metals showed moderate or weak promotional effects.[9,10] Several proposals have been offered to explain the behavior of CoMoS and NiMoS HDS catalysts: from electronic interactions that modify the reactivity of the metal components[9,11−14] to unique structural properties.[6,15,16] In these systems, the active sites probably contain CoMoS and NiMoS units.[14,17]

In recent work carried out in our laboratory,[18−21] it was demonstrated that several metals can increase the reactivity of Mo(110) toward S_2, promoting the formation of MoS_x films. A correlation was found between the formation of MoS_x in S_2/AM/Mo(110) systems (AM = Fe, Co, Ni, Cu, and Zn) and the activity of AM/MoS_2 catalysts in HDS reactions (see Figure 1).[18−20] This correlation suggests that the effects of Co and Ni on the reactivity of Mo toward sulfur-containing molecules play an important role in the high HDS activity of CoMoS and NiMoS catalysts.[18,21] In addition, Co and Ni could also enhance the HDS activity of MoS_2 by facilitating the dissociation of H_2 on the surface of the catalyst.[21,22] On molybdenum sulfide, the slow step in the H_2(gas) + S(solid) → H_2S(gas) reaction is the dissociation of molecular hydrogen.[22] Thus, if an admetal (AM) increases the concentration of atomic hydrogen on the surface of a MoS_2 catalyst, one can expect an increase in the number of unsaturated (S-free) Mo sites and in the HDS activity.

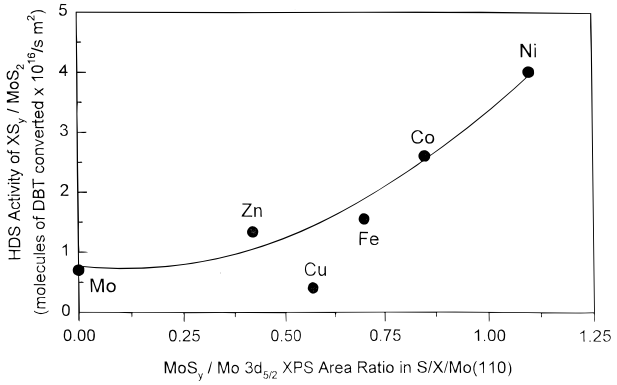

Figure 1. *x* axis: relative amount of MoS_y formed after exposing $X_{1.5}$/Mo(110) surfaces (X = Zn,[28] Cu,[29] Fe,[19] Co,[18a] and Ni;[18a] with θ_x = 1.5 monolayers) to S_2 at 700 K. *y* axis: activity of MoS_2 and metal promoted molybdenum sulfide catalysts in the desulfurization of dibenzothiophene (DBT).[9,10] The promoted catalysts were prepared using XS_y/MoS_2 mixtures (X = Zn, Cu, Fe, Co, or Ni) as precursors.[9,10]

In this article, the influence of Ni (a good HDS promoter) and Zn (a poor HDS promoter) on the reactivity of molybdenum sulfide toward hydrogen and thiophene is examined using ab initio self-consistent-field (SCF) calculations. The MoS_2-(0002)-S and $MoS_2(10\bar{1}0)$-Mo surfaces are modeled using clusters of medium size (15−26 atoms). This approach has well-known limitations,[23,24] and our main interest is in qualitative trends that can help to explain previous experimental works.

[⊗] Abstract published in *Advance ACS Abstracts,* September 1, 1997.

S1089-5647(97)01268-6 CCC: $14.00

Studies dealing with the catalytic behavior of small metal sulfide clusters have shown substantial activities and periodic trends similar to those seen for bulk metal sulfides.[25−27]

II. Theoretical Methods and Models

II. 1. Molecular Orbital Calculations. Unrestricted Hartree−Fock calculations have been carried out using the HONDO[30] and ZINDO[31] programs. Since the systems under consideration contain a large number of heavy atoms, the use of all-electron wavefunctions is not practical from a computational viewpoint. In the ab initio SCF calculations, the nonempirical effective core potentials (ECPs) of Wadt and Hay were used to describe the inner shells of the metal (Mo, Ni, Zn) and S atoms in/on the molybdenum sulfide clusters.[32,33] The ECP's for Mo included mass-velocity and Darwin relativistic effects.[33] The 5s, 5p, and 4d atomic orbitals of Mo were explicitly treated by a basis set of three s, three p, and four d primitive Gaussian-type orbitals contracted to two s, one p, and two d (3s3p4d/2s1p2d).[34] Basis sets obtained through a (3s3p5d/2s1p2d) contraction scheme were used to describe the 4s, 4p, and 3d atomic orbitals of Ni[35] and Zn.[36] The 3s and 3p orbitals of the S atoms present in the molybdenum sulfide clusters were expressed in terms of a (3s3p/2s2p) basis set.[37] The H_2 and C_4H_4S molecules were described with all their electrons, using 6-31G basis sets for C and S and a double-ζ quality basis set augmented with polarization functions for H (4s1p/2s1p).[30] Previous experience indicates that these basis sets provide satisfactory results for adsorption geometries. On the other hand, the energetics derived from these SCF calculations for adsorption reactions are not quantitative and simply provide a guide for the interpretation of experimental results. The size of the basis set, the use of finite clusters, and the lack of electron correlation introduce uncertainty in the computed binding energies.[23] In spite of this limitation, the use of ab initio SCF methods with cluster models has proved to be a very useful approach for studying a large variety of surface phenomena.[23,24]

In a set of studies, we examined the electronic properties of large clusters of Ni/MoS_2 and Zn/MoS_2 using the INDO/S method developed by Zerner and co-workers.[31,38,39] The parameters used for Mo, S, Ni, and Zn are listed in refs 31, 38 and 39. In the past, MO-SCF calculations based on this semiempirical method have provided a reliable picture for the bonding mechanism of molecules adsorbed on metal and oxide surfaces.[40] INDO/S can give qualitative information about the charge transfer associated with the chemisorption bond and the molecular orbital energy level spectrum of the adsorption complex.[40] The method has not been parameterized to provide accurate values of bond energies,[31,38,39] and, therefore, it is not useful for studying the thermochemistry of surface reactions.

II. 2. Cluster Models. Figures 2 and 3 display the clusters used to model the MoS_2(0002)-S and MoS_2(10$\bar{1}$0)-Mo surfaces. Most of these clusters have a S/Mo atomic ratio of 2, as expected for MoS_2, and they were treated as noncharged systems. Within each cluster, charge redistribution between S and Mo atoms was allowed in the MO calculations and varied depending on the number of neighbors that an atom had (see below). We will focus our attention on S or Mo atoms that form adsorption sites identical to those present in MoS_2(0002)-S and MoS_2(10$\bar{1}$0)-Mo surfaces. Clusters I (Mo_6S_{12}), II (Mo_8S_{18}), and V (Mo_5S_{10}) were employed in the ab initio SCF calculations. Clusters III ($Mo_{12}S_{24}$), IV ($Mo_{18}S_{36}$), and VI (Mo_9S_{18}) contain a relatively large number of atoms, and, therefore, their behavior was investigated with the INDO/S method. In the clusters, the Mo−S bond distances and S−Mo−S bond angles were set equal to those reported for bulk MoS_2.[41]

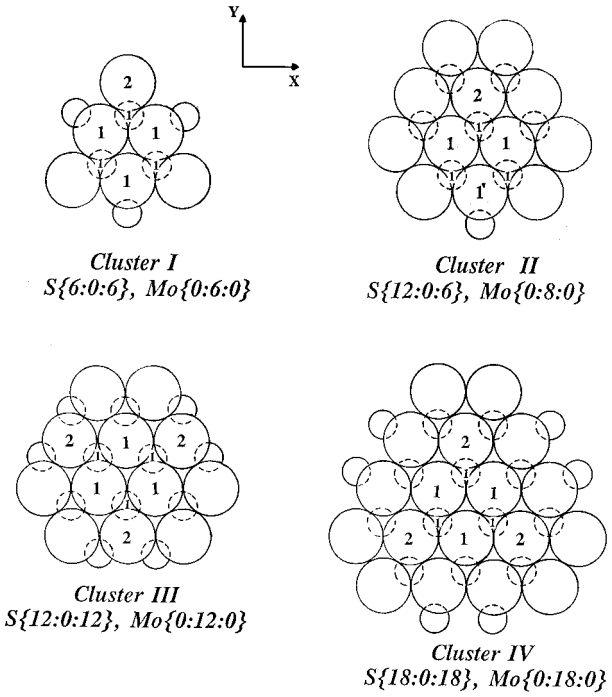

Figure 2. Clusters used to model the (0002)-S-terminated face of molybdenum disulfide: I, Mo_6S_{12}; II, Mo_8S_{18}; III, $Mo_{12}S_{24}$; and IV, $Mo_{18}S_{36}$. All the clusters have three layers, with the notation S{a:0:a} and Mo{0:a:0} specifying how many sulfur and molybdenum atoms are in each layer (a = 6−18).

The clusters in Figure 2 (MoS_2(0002)-S systems) have three layers, with the first and third containing only S atoms, and a layer of Mo atoms "sandwiched" in between. Ni and Zn atoms were adsorbed on the first layer (sulfur basal plane of MoS_2), above the three-fold hollow sites formed by the sulfur atoms labeled "1" and "2".

The clusters in Figure 3 model the Mo-terminated (10$\bar{1}$0) surface of MoS_2, which is supposed to be very active in catalytic processes.[6,7] These clusters consist of four layers, with Mo atoms in the first and third, and S atoms in the second and fourth. In these systems, we set the admetal atoms (AM = Ni or Zn) directly above the bridge sites formed by the Mo_1 atoms, Ni/MoS_2(10$\bar{1}$0) and Zn/MoS_2(10$\bar{1}$0) configurations, or along the sulfur sides on the three-fold hollow sites formed by the S_1 and S_2 atoms, Ni:MoS_2(10$\bar{1}$0) and Zn:MoS_2(10$\bar{1}$0) configurations. In the first type of configuration, the admetal can affect the properties of Mo through direct bonding. The second type of configuration is a model for a situation in which the admetal intercalates in between sulfur planes held by van der Waals forces in the layered structure of molybdenum sulfide (··SMoS··SMoS··). In this configuration, the admetal affects the properties of Mo through the S atoms to which the two metals are simultaneously bonded (AM−S−Mo). Both types of configurations are supposed to play an important role in catalytic processes.[6,7]

The AM−S or AM−Mo bond distances in clusters I, II, and V were optimized at the ab initio SCF level. The calculated values were used in the INDO/S studies for clusters III, IV, and VI. The optimal values for the AM−S bond lengths were 2.27−2.31 Å for Ni and 2.35−2.38 Å for Zn. These bond distances are similar to those seen for sulfur chemisorbed on Ni surfaces[42] and in inorganic compounds that contain S and Ni or Zn.[41a,43] For the Ni-Mo_1 and Zn-Mo_1 bond lengths in cluster V (AM/MoS_2(10$\bar{1}$0) configuration) we found values of 2.56 and 2.64 Å, respectively. These values are somewhat shorter than the sum of the corresponding metallic radii.[44]

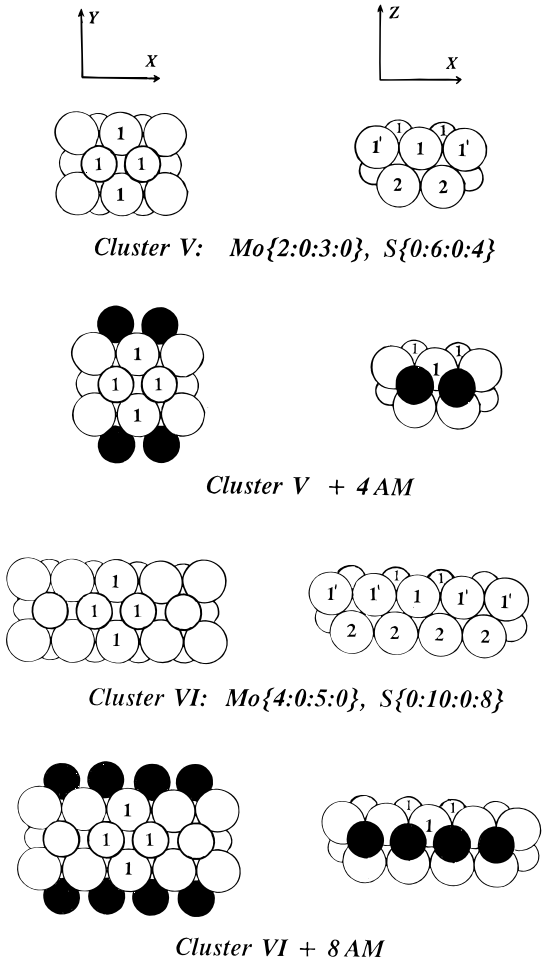

Figure 3. Top (left) and side (right) view of the clusters used to model the (10$\bar{1}$0)-Mo-terminated face of molybdenum disulfide: V, Mo_5S_{10}; and VI, Mo_9S_{18}. Both clusters have four layers, and the notation Mo-{*a*:0:*b*:0} and S{0:*c*:0:*d*} specifies how many molybdenum and sulfur atoms are in a layer. The surface normal is parallel to the *z* axis. In the studies that deal with $AM_4Mo_5S_{10}$ and $AM_8Mo_9S_{18}$ clusters, the admetal atoms were symmetrically bonded (i.e., 2 and 2, or 4 and 4) to the sulfur sides of clusters V and VI, on the three-fold hollow sites formed by combining one S_2 and two S_1 atoms (four in Mo_5S_{10}, eight in Mo_9S_{18}). In our notation, this corresponds to a AM:MoS_2(10$\bar{1}$0) configuration: a model for the intercalation of an admetal (AM) between the sulfur planes of MoS_2.

III. Results

III. 1. Interaction of Ni and Zn with MoS_2(0002) and MoS_2(10$\bar{1}$0). Figure 4 shows the calculated density of states (DOS) for cluster I (Mo_6S_{12}) at the ab initio and INDO/S levels. In qualitative terms, the agreement between the results of the two types of calculations is very good. The occupied states that appear between −6 and −16 eV contain strong contributions from the S 3p and Mo 4d atomic orbitals. The empty states located above −3.5 eV consist mainly of Mo 4d character. The left side of Figure 5 displays INDO/S results for a series of bare clusters: Mo_6S_{12} (I), Mo_9S_{18} (VI), $Mo_{12}S_{24}$ (III), and $Mo_{18}S_{36}$ (IV). Here, we can see the energy range covered by the occupied and empty "bands" of the clusters. The highest-occupied molecular orbital (HOMO) of these systems appears between −6.5 and −8 eV. Similar HOMO positions have been observed previously in ASED and DV-Xα calculations for molybdenum sulfide clusters (MoS_6^{8-}, $Mo_7S_{24}^{20-}$, Mo_3S_6, Mo_3S_{14}, and Mo_5S_{10}).[45,46] Our INDO/S and ab initio SCF calculations predict HOMO−LUMO gaps (3−4 eV) that are much larger than those seen in the ASED and DV-Xα studies (0.2−1 eV).[45,46] This discrepancy is not serious since the virtual

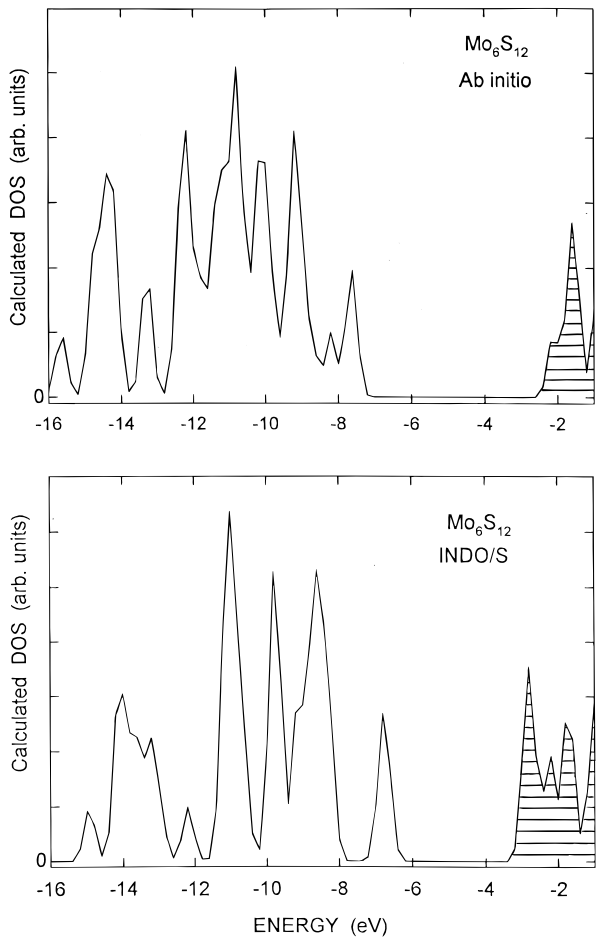

Figure 4. Calculated density of states for cluster I (Mo_6S_{12}): top, ab initio; bottom, INDO/S. The DOS plots were calculated using the discrete eigenvalue distribution from each method, broadened into bands with a Gaussian convolution as described in ref 40b (broadening parameter $\sigma = 0.15$ eV). The hatched areas indicate unoccupied states. The energies are reported with respect to the vacuum level.

(or empty) orbitals are really not well defined in any of these theoretical methods. In Figure 5, when going from Mo_6S_{12} to $Mo_{12}S_{24}$ to $Mo_{18}S_{36}$, there are only small changes in the width of the occupied "{S 3p + Mo 4d} band" and in the positions for the HOMO and LUMO of the clusters.

Experimental studies for the deposition of Ni and Zn on the sulfur basal plane of MoS_2, (0002) face, have shown that the admetals are not able to remove sulfur from molybdenum (i.e., no NiS_x or ZnS_x compound formation) remaining in a metallic state.[20,47] The Ni adatoms reduce the work function of MoS_2-(0002),[47] a phenomenon that suggests a shift in the Fermi level of the system toward the vacuum level (zero energy in Figures 4 and 5). After deposition of Ni and Zn on clusters I−VI, the ab initio and INDO/S calculations showed an increase in the energy (i.e., less negative) of the HOMOs of these systems. The graphs in the right side of Figure 5 compare the effects of Zn and Ni adatoms on the HOMO of the Mo_9S_{18} and $Mo_{18}S_{36}$ clusters (AM:MoS_2(10$\bar{1}$0) and AM/MoS_2(0002) configurations, respectively). In both cases, the electronic perturbations induced by Ni are larger than those induced by Zn. After eight Ni atoms are bonded to the sides of the Mo_9S_{18} cluster, there is a rise of almost 2 eV in the energy of the HOMO. The deposition of three Ni atoms on the $Mo_{18}S_{36}$ cluster leads to an upward shift of ∼0.5 eV in the HOMO's position. This is consistent with the results of work function measurements for the Ni/MoS_2-(0002) system.[47]

Table 1 lists calculated charges for the Mo_1 and S_1 atoms in

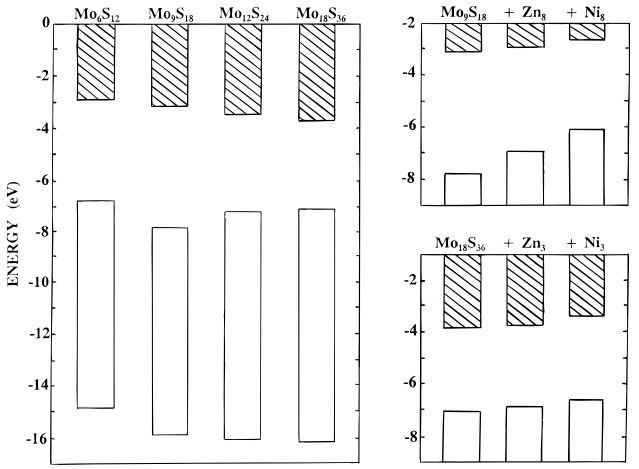

Figure 5. Results of INDO/S for a series of bare and admetal-promoted molybdenum sulfide clusters. Left: Energy range covered by the occupied and empty bands of Mo_6S_{12} (I), Mo_9S_{18} (VI), $Mo_{12}S_{24}$ (III), and $Mo_{18}S_{36}$ (IV) clusters. Right: Effects of Zn and Ni adatoms on the HOMO−LUMO gap of Mo_9S_{18} and $Mo_{18}S_{36}$. In the systems with eight adatoms, the Ni and Zn atoms were symmetrically bonded to the sulfur sides of cluster VI (4 and 4, AM:$MoS_2(10\bar{1}0)$ configuration). Three Zn or Ni atoms were deposited on the first layer of cluster IV (AM/MoS_2(0002) configuration), directly above the three hollow sites shared by one S_2 and two S_1 atoms (see Figure 2). The energies are reported with respect to the vacuum level. The hatched areas denote empty states or bands.

TABLE 1: Charges (Electrons) of Ni and Zn on MoS_2(0002)-S and $MoS_2(10\bar{1}0)$-Mo Terminated Clusters

cluster	adatom	S_1 atom	Mo_1 atom
MoS_2 (0002)-S Terminated Clusters			
cluster I[a]			
bare		−0.408	0.543
1 Ni on S_1	0.440	−0.497	0.511
1 Zn on S_1	0.324	−0.474	0.538
cluster II[a]			
bare		−0.426	0.561
1 Ni on S_1	0.382	−0.503	0.540
1 Zn on S_1	0.313	−0.484	0.547
$MoS_2(10\bar{1}0)$-Mo Terminated Cluster			
cluster V[a]			
bare		−0.542	0.426
1 Ni on Mo_1	0.271	−0.555	0.331
4 Ni on S_1,S_2	0.383	−0.653	0.311
1 Zn on Mo_1	0.194	−0.551	0.354
4 Zn on S_1,S_2	0.233	−0.598	0.343

[a] From ab initio SCF calculations. On clusters I and II, the adatom was adsorbed on the center of the hollow site formed by the sulfur atoms labeled 1 (or 1′) in Figure 2. For cluster V, a single Ni or Zn atom was adsorbed on the center of the bridge site formed by the Mo_1 atoms (see Figure 3). In the systems with four adatoms, the Ni and Zn atoms were symmetrically bonded to the sulfur sides of the cluster (2 and 2), on the hollow sites formed by the sulfur atoms present in the second and fourth layers of cluster V (AM:$MoS_2(10\bar{1}0)$ configuration).

clusters I, II, and V (bare and promoted with Zn and Ni). The values come from ab initio SCF calculations and were estimated using a Mulliken population analysis.[48,49] Due to the limitations of this type of analysis,[50,51] the charges must not be considered in quantitative terms. For the bare clusters, the calculated Mo and S charges are within the range of values observed in CNDO and DV-Xα studies of molybdenum sulfide clusters.[26,46] For example, DV-Xα calculations for Mo_3S_6, Mo_3S_{14}, and Mo_5S_{10} clusters show an average charge on Mo of 0.6 e, with individual values that vary from −0.3 to 1.5 e.[46] Tight-binding extended Huckel calculations for slabs of molybdenum disulfide show cation charges that go from 0.8 e for atoms near the surface to

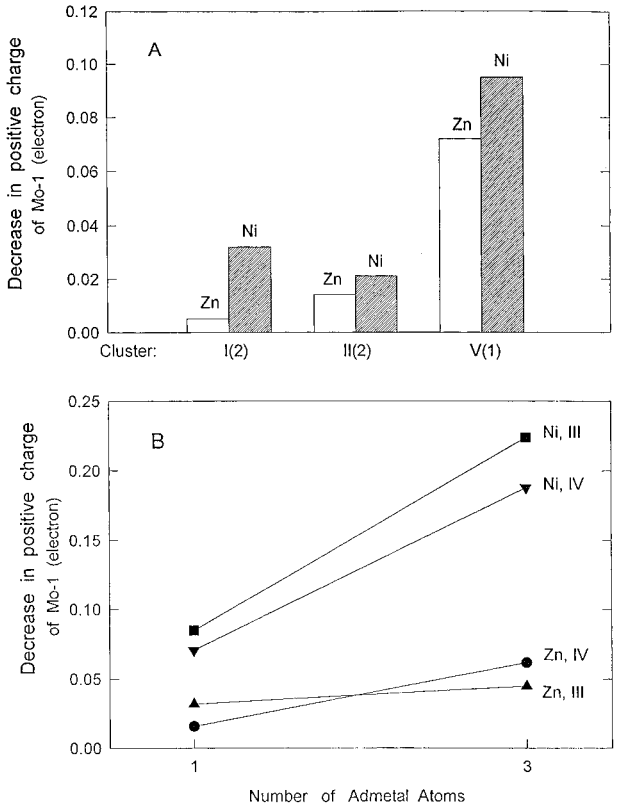

Figure 6. (A) Ni- and Zn-induced decrease in the positive charge of a Mo_1 atom in clusters I, II, and V. The results come from ab initio SCF calculations (see Table 1). The admetal atom was in the first (direct AM−Mo bonds, cluster V) or second (AM−S−Mo bonding, clusters I and II) shell of coordination of the Mo atom. (B) Decrease in the positive charge of a Mo_1 atom calculated with INDO/S[49] for the deposition of one or three admetal atoms on clusters III and IV. In the systems with one Ni or Zn atom, the admetal was on the three-fold hollow site formed by the S_1 atoms in Figure 2. For the systems with three Ni or Zn atoms, the adatoms were symmetrically located on the three hollow sites formed by one S_2 and two S_1 atoms.

1.1 e for Mo atoms in the "bulk".[11] The INDO/S and ab initio calculations for the clusters in Figures 2 and 3 show that the charge on an atom depends strongly on the number of its neighbors. If the coordination number of an atom increases, then it will be more positively charged in the case of molybdenum or more negatively charged in the case of sulfur. Conversely, if the coordination number decreases, then the atom will be less positively charged for Mo or less negatively charged for S. Identical trends are found in the DV-Xα studies mentioned above.[46]

The charges listed in Table 1 indicate that Zn and Ni should behave as electron donors when bonded to S or Mo sites of the (0002) and $(10\bar{1}0)$-Mo faces of MoS_2. Indeed, the decrease seen in the work function of MoS_2(0002) upon the deposition of Ni[47] suggests that there is a Ni→MoS_2 charge transfer. In all the adsorption cases examined, the ab initio and INDO/S results predict that nickel should be a better electron donor than zinc. In Table 1, the deposition of the admetal increases the negative charge on the S_1 atoms and reduces the positive charge on the Mo_1 atoms. Figure 6A compares the decrease in the positive charge of a Mo_1 atom upon the adsorption of a Ni or Zn atom on (0002)-S terminated clusters, I and II, and on a $(10\bar{1}0)$-Mo terminated cluster, V. Ni shows a bigger ability to electronically perturb Mo than Zn. The electronic perturbations are larger on cluster V, where there are direct admetal−Mo bonds. Figure 6B shows INDO/S results for the deposition of one or three admetal atoms on clusters III and IV. On these big systems, one sees, again, that Ni is more effective than Zn at modifying

TABLE 2: Adsorption of H on S_1, Ni, Zn, and Mo_1 Sites

Adsorption of H on S_1 Sites

cluster	bonding energy (kcal/mol)	S_1−H distance (Å)
I	−58.2	1.48
II	−52.1	1.46
V	−61.4	1.49

Adsorption of H on Ni Sites

cluster	bonding energy (kcal/mol)	Ni−H distance (Å)
Ni on I[a]	−81.6	1.62
Ni on II[a]	−85.1	1.63
Ni on V[b]	−88.9	1.61

Adsorption of H on Zn Sites

cluster	bonding energy (kcal/mol)	Zn−H distance (Å)
Zn on I[a]	−44.8	1.66
Zn on II[a]	−51.1	1.68
Zn on V[b]	−48.6	1.69

Adsorption of H on Mo_1 Sites

cluster	bonding energy (kcal/mol)	Mo−H distance (Å)
V	−69.0	1.70
V + 4Zn[c]	−72.4	1.71
V + 4Ni[c]	−78.8	1.74

[a] The adatom was on the center of the three-fold hollow site formed by the S_1 atoms of the corresponding clusters in Figure 2. [b] The adatom was on the center of the bridge site formed by the Mo_1 atoms in cluster V (see Figure 3). [c] In the systems with four adatoms, the Ni and Zn atoms were symmetrically bonded to the sulfur sides of cluster V (2 and 2), on the hollow sites formed by the sulfur atoms present in the second and fourth layer (AM:$MoS_2(10\bar{1}0)$ configuration in Figure 3).

the electronic properties of Mo. The results in Table 1 and Figure 6 are in qualitative agreement with trends found in previous studies that use less sophisticated theoretical methods or smaller cluster models.[9,11] Calculations based on the extended Huckel tight-binding method have shown that Ni atoms intercalated between the S−S planes of MoS_2 (Ni:$MoS_2(10\bar{1}0)$ configuration) reduce the positive charge on Mo atoms.[11] SCF-Xα results for $NiMoS_9^{n-}$ and $ZnMoS_9^{n-}$ clusters indicate that both admetals induce an increase in the electron density of Mo, with the effects of Ni being larger.[9] Our results support and confirm these findings.

On the basis of the electronic perturbations seen in Figures 5 and 6 (rise in the energy of the HOMO of the system and in the number of electrons on Mo centers), one can expect that Zn and Ni should modify the chemical properties of MoS_2 surfaces. This is the case for the adsorption of hydrogen and thiophene, as we will see in the following sections.

III. 2. Adsorption of H on MoS_2, Zn/MoS_2, and Ni/MoS_2 Surfaces. Experimental studies indicate that atomic hydrogen is very reactive toward molybdenum sulfide and adsorbs even on the "chemically inert" sulfur basal plane.[22] The 2H(gas) + S(surf) → H_2S(gas) reaction is very efficient for the creation of sulfur vacancies in molybdenum sulfide surfaces.[22] The ASED method has been used to study the interaction of H with a $Mo_7S_{24}^{20-}$ cluster, and values of 59−61 kcal/mol have been predicted for the adsorption energy on S sites, with the adsorption energy on Mo sites varying from 101 to 106 kcal/mol.[45] Results of density functional calculations for H chemisorption on nickel sulfide clusters (Ni_3S_2 and Ni_3S_3) show adsorption energies of 43−61 kcal/mol on the Ni centers.[27]

Table 2 shows ab initio SCF results for the adsorption of a H atom on clusters I, II, and V (bare and promoted with Ni and Zn). At the top of the table are listed calculated bonding energies (52−61 kcal/mol) and bond distances (1.46−1.49 Å) for H adsorption on S_1 sites of the bare clusters. These values are in close agreement with those found in the ASED studies mentioned above.[45] The ab initio results for H on clusters I and II showed an increase of 3−7 kcal/mol in the hydrogen bonding energy when the adatom was moved from a S_1 atom to S atoms at the edge of the cluster. This is consistent with the common notion that S edge atoms should be the easiest to hydrogenate and remove from molybdenum sulfide surfaces. We found a drastic reduction in the hydrogen adsorption energy when the coverage of hydrogen on clusters I and II was increased. Figure 7 shows how the average H adsorption energy changes after depositing one, two, and three H atoms on one, two, and three S_1 sites of clusters I and II. There is a decrease of 14−23 kcal/mol in the H adsorption energy when going from one to three adatoms. The magnitude of this decrease was reduced to 8−12 kcal/mol when H atoms were shifted to the S edges of the clusters. These results suggest that it should be much easier to accumulate significant amounts of hydrogen on the edges of a MoS_2(0002)-S surface than on the terrace sites, facilitating, in this way, the hydrogenation and removal of S edge atoms.

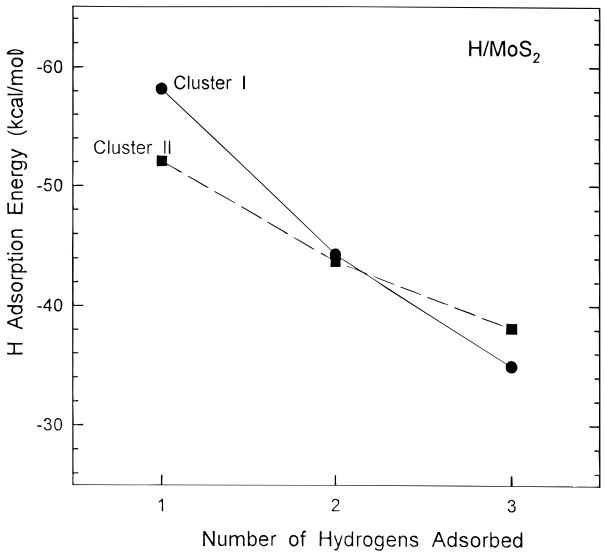

Figure 7. Effect of coverage on the adsorption energy of atomic hydrogen on clusters I and II. The values reported correspond to an average of the H adsorption energy in systems with one, two and three adatoms. Each H atom was adsorbed on a different sulfur atom. The sequence in which the sulfur sites were occupied was: 1, 1 + 1, and 1 + 1 + 1 (I) or 1 + 1 + 1′ (II). The total adsorption energies were calculated at the ab initio SCF level, optimizing the H−S bond lengths.

By depositing Zn or Ni on MoS_2(0002)-S, one "creates" metal centers on which H can adsorb, and the overall reactivity of the system, in principle, may increase. In Table 2 are listed calculated bonding energies and bond distances for the adsorption of a H atom on Ni and Zn atoms supported on clusters I, II, and V. The results come from ab initio SCF calculations. The calculated H adsorption energies on MoS_2-supported Ni (82−89 kcal/mol) are somewhat larger than those observed in density functional calculations for the adsorption of H on metal sites of nickel sulfide clusters (43−61 kcal/mol).[27] This difference could be easily a consequence of comparing results from two different theoretical approaches,[23,24] instead of reflecting real changes in the chemical properties of the Ni atoms. In Table 2, the Ni ↔ H interactions are considerably stronger than the Zn ↔ H or S ↔ H interactions. The deposition of Zn on (0002)-S terminated clusters, I and II, does not lead to an improvement in the H chemisorption ability of these systems.

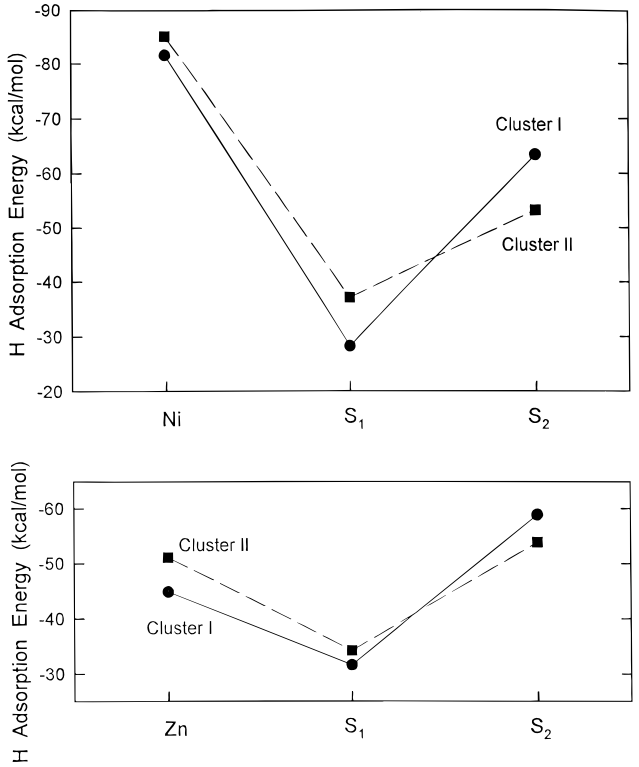

Figure 8. Adsorption energy at the ab initio SCF level for a hydrogen atom on Mo_6S_{12} (I) and Mo_8S_{18} (II) clusters promoted with Ni (top panel) and Zn (bottom panel). In these systems, an admetal atom was positioned on the hollow site formed by the S_1 atoms (see Figure 2). Then, the hydrogen atom was set directly above each adsorption site (Ni, Zn, S_1, or S_2), and the H−cluster and admetal−cluster distances were optimized.

Figure 8 shows how the adsorption energy varies when the H adatom is moved from the admetal to sulfur sites in clusters I and II. From a thermodynamic viewpoint, the migration of H from Ni to S is much more difficult than the migration from Zn to S. In the calculations of Figure 8, the admetal was bonded to the S_1 sites of the clusters, and this bonding deactivated these sulfur sites toward H chemisorption (they became coordinatively saturated). For the systems in Figure 8, the H adsorption energy on S_1 sites was 13−29 kcal/mol smaller than those on the corresponding sites of the bare clusters. On the other hand, the presence of the admetal had a very minor effect on the S_2↔H interactions (adsorption energy changes <5 kcal/mol). This is due to the fact that these sulfur sites were well separated from the admetal (∼3.9 Å, third nearest neighbors).

At the bottom of Table 2 are shown the bonding energy and bond distance calculated for the adsorption of a H atom on a Mo_1 site of cluster V ($MoS_2(10\bar{1}0)$-Mo surface). The bonding energy (69 kcal/mol) is smaller than those found in ASED calculations for a H atom bonded to Mo sites of a $Mo_7S_{24}^{20-}$ cluster (101−106 kcal/mol).[45] Experiments for the interaction of H with molybdenum sulfide films that are rich in sulfur vacancies show desorption of H_2 at temperatures (350−600 K) consistent with Mo−H bonding energies of 65−80 kcal/mol.[22] Our ab initio SCF results are probably in fortuitous agreement with these experimental data. For a molybdenum sulfide cluster, one can expect a reactivity larger than that for a $MoS_2(10\bar{1}0)$-Mo surface, but, due to the lack of electron correlation, the SCF calculations should underestimate bonding energies. These two "defects" probably cancel each other, and the computed H adsorption energies on cluster V are close to those observed experimentally for H on molybdenum sulfide surfaces.[22] In Table 2, when Ni or Zn is added to the sulfur sides of cluster V (AM:$MoS_2(10\bar{1}0)$ configuration), there is a significant increase (3−10 kcal/mol) in the strength of the Mo_1↔H interactions. Ni is more effective than Zn at enhancing the reactivity of Mo toward H. This correlates with the results of Figures 5 and 6, where nickel induces the largest electronic perturbations on the molybdenum sulfide clusters.

TABLE 3: H_2 Adsorption on $MoS_2(0002)$

	adsorption energy (kcal/mol)	S_1−H bond (Å)	H−H bond (Å)
free H_2			0.73
on cluster I			
S_1, H−H vertical	−0.4	1.58	0.75
S_1, parallel	−0.3	1.63	0.74
S_1,S_1 (2H)	−3.6	1.49	3.16
on cluster II			
S_1, vertical	−0.5	1.59	0.74
S_1, parallel	−0.3	1.65	0.73
S_1,S_1 (2H)	−2.7	1.47	3.16
S_1,S_2 (2H)	−2.9	1.48, 1.47	3.16

TABLE 4: H_2 Adsorption on $Ni/MoS_2(0002)$ and $Zn/MoS_2(0002)$[a]

	adsorption energy (kcal/mol)	admetal−H bond (Å)	S−H bond (Å)	H−H bond (Å)
on $NiMo_8S_{18}$				
Ni, H−H vertical	−11.4	1.68		0.79
Ni, parallel	−13.8	1.73		0.82
Ni,S_1 (2H)	−19.6	1.64	1.51	2.42
Ni,S_2 (2H)	−37.3	1.62	1.47	3.99
on $ZnMo_8S_{18}$				
Zn, vertical	−1.5	1.74		0.76
Zn, parallel	−0.6	1.79		0.76
Zn,S_1 (2H)	+8.8	1.68	1.53	2.47
Zn,S_2 (2H)	−11.7	1.66	1.48	4.03

[a] The admetal atom was located on the center of the three-fold hollow site formed by the S atoms labeled 1 and 1′ in cluster II (see Figure 2).

III. 3. Adsorption of H_2 on MoS_2, Zn/MoS_2, and Ni/MoS_2 Surfaces. On molybdenum sulfide, the slow step in the H_2-(gas) + S(solid) → H_2S(gas) reaction is the dissociation of molecular hydrogen.[22] In principle, if a metal promoter raises the concentration of atomic hydrogen on the surface of a MoS_2 catalyst, one can expect an increase in the number of unsaturated (or S-free) Mo sites and in the HDS activity of the system.[22] We will begin this section with studies dealing with the interaction of H_2 with bare and admetal-promoted $MoS_2(0002)$ surfaces. This will be followed by a presentation of similar studies for $MoS_2(10\bar{1}0)$ and AM:$MoS_2(10\bar{1}0)$ systems.

Table 3 shows ab initio SCF results for the adsorption of H_2 on top of S_1 sites of clusters I and II. The molecule was oriented with its H−H axis either vertical or parallel to the sulfur basal plane (*xy* plane in Figure 2). In both cases, the H_2 adsorption energy was negligible. During the dissociation of H_2 on the sulfur sites, only a very small amount of energy (2.7−3.6 kcal/mol) was released. These results agree with experimental data which indicate that the sulfur basal plane of MoS_2 is essentially inert toward molecular hydrogen.[22,52] Adsorption and reaction with H_2 have been observed only at temperatures above 800 K.[52]

In Table 4 are shown ab initio SCF results for the interaction of a H_2 molecule with Ni and Zn atoms supported on cluster II ($NiMo_8S_{18}$ and $ZnMo_8S_{18}$ systems, respectively). As usual, the admetal atom was located on the three-fold hollow site shared by the sulfur atoms labeled 1 and 1′ in Figure 2. On a supported Ni atom, the H_2 adsorption energy (∼14 kcal/mol) is much larger than that on S_1 sites of the bare cluster (∼0.5 kcal/mol) and comparable to bonding energies observed in density

TABLE 5: H_2 Adsorption on $MoS_2(10\bar{1}0)$, Ni:$MoS_2(10\bar{1}0)$, and Zn:$MoS_2(10\bar{1}0)$

	adsorption energy (kcal/mol)	Mo_1−H bond (Å)	H−H bond (Å)
on Mo_5S_{10}			
Mo_1, vertical	−8.6	1.76	0.78
Mo_1, parallel	−10.2	1.80	0.79
Mo_1,Mo_1 bridge	−13.6	1.83	0.82
Mo_1,S_1 (2H)[b]	−27.1	1.72	2.49
Mo_1,Mo_1 (2H)	−39.4	1.69	3.16
on $Zn_4Mo_5S_{10}$[a]			
Mo_1, vertical	−8.8	1.77	0.79
Mo_1, parallel	−10.5	1.80	0.81
Mo_1,Mo_1 bridge	−14.1	1.82	0.82
Mo_1,Mo_1 (2H)[b]	−41.7	1.73	3.16
on $Ni_4Mo_5S_{10}$[a]			
Mo_1, vertical	−10.4	1.76	0.79
Mo_1, parallel	−12.2	1.81	0.84
Mo_1,Mo_1 bridge	−16.3	1.84	0.86
Mo_1,Mo_1 (2H)[b]	−50.3	1.72	3.16

[a] The Ni and Zn atoms were symmetrically bonded to the sulfur sides of cluster V (2 and 2) on the hollow sites formed by the sulfur atoms present in the second and fourth layers. [b] 2H denotes two separated H atoms adsorbed on the indicated sites: Mo_1 and S_1, or the two Mo_1 atoms in cluster V.

functional calculations for H_2↔Ni interactions on nickel sulfide clusters (9−15 kcal/mol).[27] In the case of supported Zn, the H_2 adsorption energy is relatively small (∼1.5 kcal/mol) and close to that seen for S_1 atoms in the bare cluster. In Table 4 are also listed ΔE values for the dissociative adsorption of H_2, with a H atom remaining on the admetal and the other moving to a S_1 or S_2 site in the cluster. The reader should keep in mind that the S_1 atoms are bonded to Ni or Zn and, therefore, are less efficient for H bonding than the S_2 atom (see Figure 8). For the dissociation of H_2, the energy released on the $NiMo_8S_{18}$ cluster (20−37 kcal/mol) is much larger than that on the unpromoted Mo_8S_{18} cluster (∼2.8 kcal/mol). On the $NiMo_8S_{18}$ system, the dissociation of H_2 is highly exothermic, even when a H atom "lands" on a S_1 site. The large strength of the Ni−H bond carries the energetics of the dissociation process. On the other hand, in the case of $ZnMo_8S_{18}$, the Zn−H bond is relatively weak, and the dissociation of H_2 becomes exothermic only when the S_2 atom is involved in the process. The results in Table 4 indicate that Ni should be much better than Zn as a source of atomic hydrogen ($H_{2,gas} \rightarrow 2H_{adsorbed}$) on the sulfur basal plane of molybdenum sulfide.

Now, we will shift our attention to the interaction of H_2 with the $(10\bar{1}0)$-Mo terminated face of MoS_2 which is supposed to play a very important role in HDS catalysis.[6,7] Table 5 displays ab initio SCF results for the adsorption of H_2 on cluster V: bare, Mo_5S_{10}, and promoted with Zn and Ni adatoms in a AM: $MoS_2(10\bar{1}0)$ configuration, $Zn_4Mo_5S_{10}$ and $Ni_4Mo_5S_{10}$. In these studies, the hydrogen molecule was adsorbed on top of a Mo_1 site, with its H−H axis vertical or parallel to the surface, or bridging two Mo_1 atoms in a Mo−H−H−Mo conformation. The stability of these adsorption geometries increased in the following sequence: a-top H−H vertical < a-top H−H parallel < bridge H−H parallel. For a-top adsorption, the most stable configuration involved a H−H bond parallel to the surface and oriented along the *y* axis in Figure 3 (i.e., two equivalent Mo_1−H bonds with the hydrogen atoms pointing toward the sulfur sides of the cluster). In this configuration, a barrier of 1.3−2.1 kcal/mol was found for the rotation of the H−H bond around the surface normal. H_2 adsorption geometries in which both H atoms are simultaneously bonded to Mo are probable precursors for the dissociation of the molecule. In these configurations, the adsorption of the molecule leads to a significant increase (0.06−0.09 Å) in the H−H bond length (0.73 Å in free H_2).

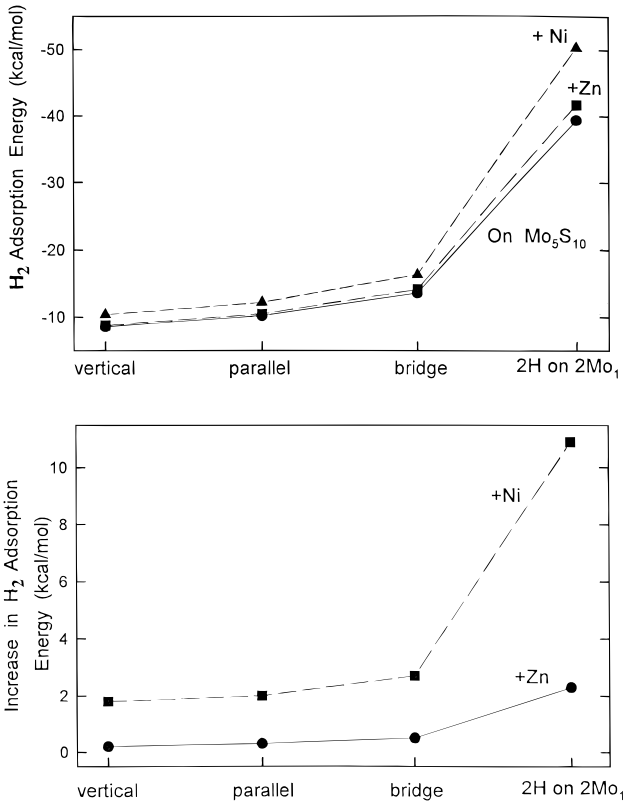

Figure 9. Top: Hydrogen adsorption energies on clusters modeling the clean and promoted $MoS_2(10\bar{1}0)$-Mo surface: Mo_5S_{10} (●), $Zn_4Mo_5S_{10}$ (■), and $Ni_4Mo_5S_{10}$ (▲). The Zn and Ni adatoms were symmetrically bonded to the S sides (2 and 2) of cluster V. H_2 was adsorbed on top of a Mo_1 atom (H−H bond vertical or parallel to the surface) or bridging two Mo_1 atoms in a Mo−H−H−Mo configuration. For comparison, the results for the adsorption of two H atoms on two Mo_1 atoms are also included. Bottom: Increase induced by the Zn and Ni adatoms on the hydrogen bonding energies (H_2/Mo_5S_{10} − $H_2/Zn_4Mo_5S_{10}$; H_2/Mo_5S_{10} − $H_2/Ni_4Mo_5S_{10}$).

On a bare Mo_5S_{10} cluster, the dissociation of H_2 is a very exothermic reaction. This is in clear contrast with the energetics for the dissociation of the molecule on (0002)-S-terminated clusters (see Table 3).

When Ni and Zn are added to the sulfur sides of cluster V, one sees a rise in the strength of the Mo_1↔H_2 interactions and in the ΔE for dissociative chemisorption. Figure 9 compares the effects of the admetals on the adsorption energies for H_2 and two H atoms on cluster V. By far, Ni induces the largest increases in the hydrogen bonding energies. These effects are very pronounced for the adsorption of atomic hydrogen ($H_{2,gas} \rightarrow 2H_{adsorbed}$). In general, Ni produces increases of 19−25% in the ΔE associated with the adsorption or dissociation of the H_2 molecule, whereas increases induced by Zn are in the range of 3−6%.

Since the presence of Ni has such a large effect on the energetics for H_2 dissociation on Mo, it is worthwhile to examine the interaction of H_2 with the Mo_5S_{10} and $Ni_4Mo_5S_{10}$ clusters in more detail. Figure 10 shows the energy profile associated with the dissociation of H_2 on a Mo_1 site of Mo_5S_{10} and $Ni_4Mo_5S_{10}$. In the "initial state" of these systems, H_2 was in the optimized structure for molecular adsorption (see Table 5). H_2 was adsorbed with its molecular axis parallel to the surface (two equivalent Mo_1-H bonds) and the hydrogens pointing toward the sulfur sides of the cluster (along the y axis in Figure 3). The results in Figure 10 indicate that there is an energy barrier for the dissociation of H_2 on a Mo_1 site. On Mo_5S_{10}, the size of the barrier is ∼6 kcal/mol, and in the "transition state" (i.e.,

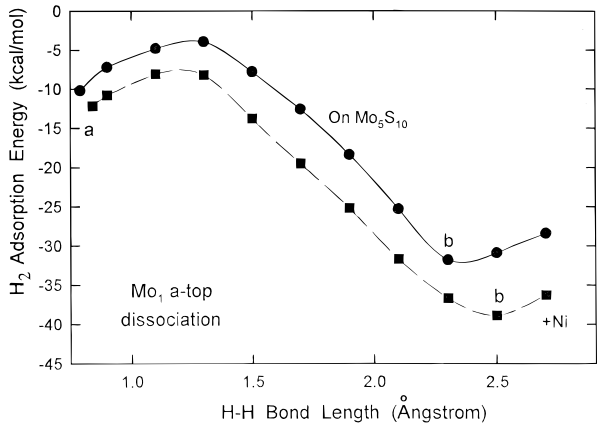

Figure 10. Dissociation of H_2 on $Ni_4Mo_5S_{10}$ and Mo_5S_{10} (cluster V). H_2 was adsorbed on a Mo_1 atom with its molecular axis parallel to the $(10\bar{1}0)$ surface and the hydrogens pointing toward the sulfur sides of the cluster (along the *y* axis in Figure 3). The H−H bond was elongated, and the two equivalent Mo_1−H distances were optimized. The initial configurations (point a) were H−H = 0.79 Å, Mo_1−H = 1.80 Å for Mo_5S_{10}, and H−H = 0.84 Å, Mo_1−H = 1.81 Å for $Ni_4Mo_5S_{10}$. At the minima (point b), the configurations were H−H = 2.30 Å, Mo_1−H = 1.71 Å for Mo_5S_{10}, and H−H = 2.50 Å Mo_1−H = 1.73 Å for $Ni_4Mo_5S_{10}$. The adsorption energy was calculated using the corresponding isolated cluster and the free H_2 molecule as reference state.

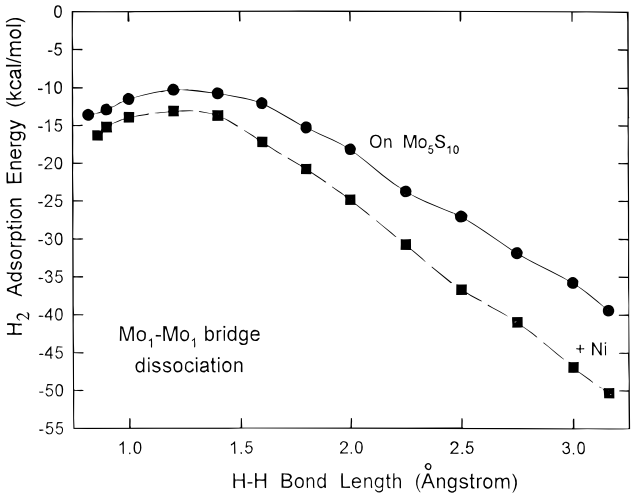

Figure 11. Dissociation of H_2 on Mo_5S_{10} and $Ni_4Mo_5S_{10}$. H_2 was adsorbed on the center of the bridge between the two Mo_1 atoms in cluster V. The H−H axis of the molecule was parallel to the $(10\bar{1}0)$ surface and oriented along the *x* axis in Figure 3. The H−H bond was elongated, and the two equivalent Mo_1−H bond distances were optimized. The Mo_1−H bond lengths for the initial (H_2 adsorption) and final (two H atoms adsorbed) configurations of these systems are shown in Table 5. The adsorption energy was calculated using the corresponding isolated cluster and the free H_2 molecule as reference state.

top of the barrier), the molecule is weakly bound to the surface, favoring desorption instead of dissociation of H_2. After adding Ni to the cluster, there is a small reduction in the size of the energy barrier and a significant enhancement in the adsorption energy for the transition state. These effects, together with an increase in the stability of the final products, make much easier the dissociation of the H_2 molecule.

Figure 11 displays the calculated energy profile for the dissociation of H_2 on two Mo_1 sites of Mo_5S_{10} and $Ni_4Mo_5S_{10}$ (Mo−H−H−Mo initial configuration). In these cases, the energy barriers are smaller and the transition states more stable than those for the dissociation of the molecule on a single Mo_1 atom. Thus, on $MoS_2(10\bar{1}0)$-Mo surfaces, H−H bond cleavage should occur faster on bridge than on a-top Mo_1 sites. On bridge

TABLE 6: Thiophene Adsorption on Ni/MoS_2(0002) and Zn/MoS_2(0002)[a]

	adsorption energy (kcal/mol)	AM-S (Å)	AM-C_α (Å)	AM-C_β (Å)
On $NiMo_6S_{12}$				
η^1	−9.2	2.34		
η^5	−16.8	2.39	2.24	2.19
on $ZnMo_6S_{12}$				
η^1	−4.9	2.41		
η^5	−6.4	2.45	2.30	2.23

[a] AM = admetal, Ni or Zn. Figure 12a shows the orientation of the thiophene molecule in η^1- and η^5-coordination modes.

Mo sites, Ni again favors the dissociation of H_2 by stabilizing the transition state and final products of this reaction. The electronic perturbations that Ni induces on Mo (see Figures 5 and 6) make the Mo atoms better electron donors, facilitating a charge transfer from the surface into the antibonding $1\sigma_u$ orbital of H_2 that leads to dissociation of the molecule.

In summary, it has been shown in this section that Ni and Zn can increase the coverage of H on the surface of a MoS_2 catalyst by providing sites for the dissociation of H_2 on (0002)-S-terminated terraces and by increasing the reactivity of Mo toward H_2. Our theoretical studies indicate that Ni should be much more efficient than Zn for promoting the $H_{2,gas} \rightarrow 2H_{adsorbed}$ reaction.

III. 4. Thiophene Adsorption on MoS_2, Zn/MoS_2, and Ni/MoS_2. Thiophene is frequently used as a test molecule in HDS studies.[6−8,11,26,27,40d,46,53,54] From a computational viewpoint, thiophene (C_4H_4S) is a much more complex and demanding molecule than H_2. This makes it difficult to deal with thiophene at an ab initio SCF level: to compensate for the large size of the basis set necessary to describe the behavior of the adsorbate, one has to limit the size of the clusters used to model the surface. In the ab initio studies discussed in this section, the (0002)-S and $(10\bar{1}0)$-Mo faces of MoS_2 were modeled using clusters I and V, respectively. In a few cases, qualitative trends for the adsorption of thiophene were also examined employing the INDO/S method and clusters IV and VI.

After optimizing the geometry of the free C_4H_4S molecule at the ab initio SCF level, we found bond distances (C_α−S = 1.78 Å; C_α−C_β = 1.34 Å; C_β−C_β = 1.45 Å) and bond angles that are very close to those observed in experiments of electron diffraction.[55] In general, the adsorption process produced very small changes in the geometry of the molecule.

The ab initio SCF calculations showed small bonding energies for the interaction of thiophene with a S_1 atom of cluster I: 3.7 kcal/mol for bonding through the S end of the molecule (aromatic ring perpendicular to the surface) and 2.9 kcal/mol for bonding through the aromatic ring. These values are smaller than the value of 9.5 kcal/mol reported for the adsorption energy of thiophene on MoS_2(0002).[56] Table 6 shows ab initio results for the adsorption of thiophene on a Ni or Zn atom supported on cluster I. The admetal was set above the hollow site formed by the S_1 atoms in Figure 2, and the C_4H_4S molecule was bonded in the two coordination modes displayed in Figure 12a. In these configurations, the energy barrier for rotation of the molecule around the surface normal was small (<0.8 kcal/mol). On the $NiMo_6S_{12}$ and $ZnMo_2S_{12}$ clusters, thiophene exhibits the strongest adsorbate−substrate interactions in a η^5 configuration. An identical result was found in INDO/S calculations for the adsorption of thiophene on a Ni atom supported on cluster IV ($NiMo_{18}S_{36}$)[60] and in density functional calculations that deal with the bonding of the molecule to metal sites of nickel sulfide clusters.[27] This density functional calculations show bonding energies (20−29 kcal/mol) that are somewhat

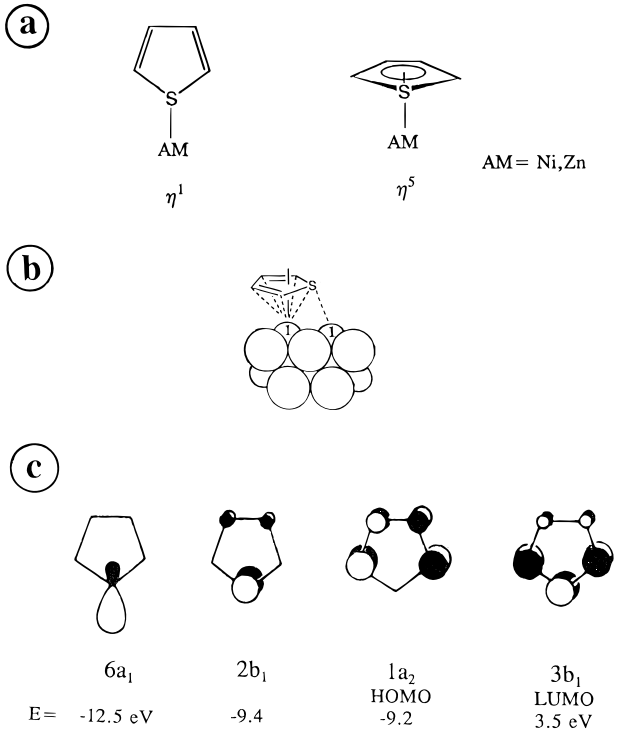

Figure 12. (a) η^1- and η^5-coordination modes for thiophene on a Ni or Zn adatom. (b) Most stable bonding geometry for thiophene on cluster V (η^5 coordination in Table 7). (c) Rough picture for the S lone pairs ($6a_1$ and $2b_1$), HOMO ($1a_2$), and LUMO ($3b_1$) of thiophene.[11,57] The displayed MO energies come from our ab initio SCF calculations and are close to those found with the INDO/S method.[58] The experimental ionization potentials for the $6a_1$, $2b_1$, and $1a_2$ orbitals of thiophene are 12.1, 9.5, and 8.9 eV, respectively.[59]

TABLE 7: Thiophene Adsorption on $MoS_2(10\bar{1}0)$, Ni/$MoS_2(1010)$, and Zn/$MoS_2(1010)$

	adsorption energy (kcal/mol)	M−S[a] (Å)	M−C_α[a] (Å)	S−C_α (Å)	C_α−C_β (Å)
free				1.78	1.34
on Mo_5S_{10}					
η^1 a-top	−11.2	2.46		1.78	1.33
η^1 bridge	−14.9	2.49		1.79	1.34
η^5	−21.4	2.54	2.39	1.83	1.40
on $NiMo_5S_{10}$					
η^1 a-top	−8.6	2.32		1.78	1.35
η^5 a-top	−19.3	2.42	2.25	1.81	1.38
on $ZnMo_5S_{10}$					
η^1 a-top	−5.3	2.40		1.78	1.34
η^5 a-top	−7.7	2.47	2.31	1.79	1.33

[a]M corresponds to Mo_1 in Mo_5S_{10}, Ni in $NiMo_5S_{10}$, and Zn in $ZnMo_5S_{10}$. The admetal atom was set on the bridge between the two Mo_1 atoms in cluster V (see Figure 3). Thiophene was bonded to the admetal in the coordination modes shown in Figure 12a.

bigger than the adsorption energies shown in Table 6 for thiophene on a supported Ni atom (9−17 kcal/mol). A comparison of the ab initio results for C_4H_4S on $NiMo_6S_{12}$ and $ZnMo_6S_{12}$ clusters suggests that Ni should be much more effective than Zn for activating the $MoS_2(0002)$ surface toward thiophene chemisorption.

At the top of Table 7 are listed ab initio results for the bonding of thiophene to cluster V in three different coordination modes. In the η^1 configurations, the molecule was adsorbed with the aromatic ring perpendicular to the surface and the sulfur end on top of a Mo_1 site or on the center of the bridge between the two Mo_1 sites. For a η^1-top coordination, the largest adsorption energy was found when the molecular plane of thiophene was parallel to the *xz* plane in Figure 3, and there was an energy barrier of ∼1.4 kcal/mol for rotation of the molecule around the surface normal. In a η^1-bridge coordination, the most stable orientation was with the aromatic ring parallel to the *yz* plane, and the barrier for rotation was close to 4 kcal/mol. This orientation maximizes the interaction between the $C_4H_4S(2b_1)$ orbital (a pseudo-lone-pair orbital, see Figure 12c) and the two Mo_1 atoms to which the molecule is bonded. Finally, the molecule was adsorbed with its molecular plane parallel to the surface (η^5 coordination). In this case, the aromatic ring was positioned above one of the Mo_1 atoms, with the S end of the molecule pointing toward the second Mo_1 atom (see Figure 12b). Such a orientation allows for the interaction of the "sulfur lone-pairs" of the molecule ($2b_1$ and $6a_1$ orbitals, see Figure 12c) with the second Mo_1 atom. The optimization of this geometry produced S−Mo_1 distances of 2.54 (Mo_1 atom with the aromatic ring on top) and 2.61 Å (second Mo_1 atom), which indicate that thiophene was bonded to both metal atoms. This configuration was very stable, and rotation of the molecule around the surface normal was prevented by an energy barrier of ∼7.8 kcal/mol. In Table 7, the adsorption energies for thiophene on Mo_5S_{10} increase in the following sequence: η^1-top < η^1-bridge < η^5 . According to these results, thiophene should adopt a η^5 coordination on $MoS_2(10\bar{1}0)$-Mo surfaces. An identical conclusion can be reached by analyzing the bonding interactions between thiophene and cluster VI in several conformations using the INDO/S method. Previous results of extended Huckel[11,61] and CNDO[26] calculations also indicate that thiophene prefers to adopt an η^5 coordination when bonded to Mo in molybdenum sulfide clusters.

In Table 7, it is interesting to notice that adsorption of thiophene on Mo_5S_{10} in η^1 configurations produces negligible changes in the geometry of the ring. Significant structural changes are only found in a η^5 coordination, which is frequently postulated as a precursor for hydrogenation of the ring and C−S bond breaking in HDS reactions.[6,11,26] This configuration maximizes the interactions of the HOMO and LUMO of thiophene ($1a_2$ and $3b_1$ orbitals, see Figure 12c) with the metal site. The LUMO or $3b_1$ orbital is S−C_α and C_α−C_β antibonding. Partial population of this orbital by interaction with an active site will cause a weakening and elongation in the S−C_α and C_α−C_β bonds.

In a set of studies, we investigated the effects of Ni and Zn on the strength of the C_4H_4S−Mo bonds by adding two atoms of these admetals to one of the sulfur sides of cluster V (AM: $MoS_2(10\bar{1}0)$ geometry). The adatoms were positioned on the hollow sites formed by the S_1 and S_2 atoms, one "in front" of each Mo_1 atom (see Figure 3). These model clusters ($Ni_2Mo_5S_{10}$ and $Zn_2Mo_5S_{10}$) represent the intercalation of a promoter between the sulfur planes in the layered structure of MoS_2 (••SMoS••SMoS••). In previous works, it has been proposed that this intercalation could lead to an enhancement in the strength of the C_4H_4S−Mo bond by modifying the chemical properties of molybdenum through Mo−S−AM interactions.[7,11] Indeed, thiophene adsorbed on Mo_1 sites of $Ni_2Mo_5S_{10}$ exhibited bonding energies that were bigger than those seen on Mo_5S_{10}, with increases of 1.4, 2.6, and 2.3 kcal/mol for η^1-top, η^1-bridge, and η^5 coordinations, respectively. On the other hand, for the adsorption of C_4H_4S on Mo_1 sites of $Zn_2Mo_5S_{10}$, the bonding energies were almost equal (±0.6 kcal/mol) to those found on Mo_5S_{10}. Thus, Ni seems to be much better than Zn for enhancing C_4H_4S↔Mo interactions. The results in Table 6 indicate that Ni supported on a (0002)-S surface adsorbs thiophene stronger than supported Zn. An identical trend is seen in Table 7 for the adsorption of thiophene on Ni and Zn atoms supported on Mo_1 sites of cluster V ($NiMo_5S_{10}$ and $ZnMo_5S_{10}$, both in a AM/$MoS_2(10\bar{1}0)$ configuration). The

adsorption energies on supported Ni are comparable to those on Mo_1 sites. On the basis of the results analyzed in this section, one can expect stronger C_4H_4S↔Mo and C_4H_4S↔AM interactions in NiMoS catalysts than in ZnMoS catalyst.

IV. Discussion

The ab initio and INDO/S studies presented above indicate that Ni induces important changes in the electronic and chemical properties of large clusters that resemble the MoS_2(0002)-S and $MoS_2(10\bar{1}0)$-Mo surfaces. In contrast, the perturbations induced by Zn are relatively small. Our results are consistent with those of previous calculations based on the tight-binding extended Huckel[11] and Xα[9,12] methods, which show Ni-induced changes in the electronic properties of slabs and small clusters of molybdenum sulfide. The data in section III for the promoted $MoS_2(10\bar{1}0)$-Mo surface show a simultaneous increase in the electron density on Mo and in the reactivity of this metal toward H_2 and thiophene. In addition, Ni and Zn enhance the chemical activity of MoS_2(0002)-S by providing active sites for the dissociation of H_2 and the chemisorption of thiophene.

Several catalytic processes (hydrogenation of olefins,[4] synthesis of alcohols from CO,[3] HDS and HDN reactions[5−8]) depend on the interaction of H_2 with MoS_2. Studies of scanning transmission microscopy have revealed that the sulfur basal plane of MoS_2 is virtually unreactive toward H_2.[52] Hydrogen attacks only the edge planes of MoS_2.[52] This behavior agrees with trends found in the energetics for the dissociation of H_2 on MoS_2(0002)-S and $MoS_2(10\bar{1}0)$-Mo clusters (Tables 3 and 5). Our results indicate that there is an energy barrier (4−6 kcal/mol) for the dissociation of H_2 on $MoS_2(10\bar{1}0)$-Mo. On this surface, H_2 dissociation should be faster on bridge Mo sites than on a single Mo atom. Zn produces only minor changes in the energetics for H−H bond cleavage on $MoS_2(10\bar{1}0)$-Mo. On the other hand, Ni largely raises the probability for H_2 dissociation by substantially increasing the stability of the transition state and products of this reaction (Figures 10 and 11). In the case of MoS_2(0002)-S clusters, the dissociative adsorption of H_2 is much more exothermic on Ni-promoted surfaces than on clean or Zn-promoted surfaces (Tables 3 and 4). This is consistent with trends found in experimental studies: at 300 K, under ultrahigh-vacuum conditions, H_2 dissociates on Ni/MoS_2(0002),[18b,21] whereas no dissociation or adsorption of the molecule is observed on Zn/MoS_2(0002) or MoS_2(0002).[20,22]

On molybdenum sulfide, the slow step in the creation of unsaturated metal sites through the H_2(gas) + S(surface) → H_2S-(gas) reaction is the dissociation of molecular hydrogen.[22] Thus, if a metal promoter enhances the coverage of atomic hydrogen on the surface of a MoS_2 catalyst, one can expect an increase in the number of unsaturated Mo sites and in the catalytic activity. Following this line of thought, the results in section III.3 indicate quite clearly that Ni should be an excellent promoter, while the effects of Zn on the catalytic activity should be small.

The industrial HDS catalysts are complex systems, in which molybdenum sulfide coexists with different promoters on a γ-alumina support[6−8] The exact nature of the active sites in these catalysts is not known, and various "models" have been offered to explain their behavior.[6−8,17] In a study examining the effects of several metal promoters on the hydrodesulfurization of dibenzothiophene over molybdenum sulfide catalysts,[9,10] it was found that the enhancement in the catalytic activity induced by Ni was ∼3 times larger than that produced by Zn. Figure 1 compares trends observed in the HDS activity of these promoted molybdenum sulfide catalysts (XS_y/MoS_2 catalyst precursor; X = Zn, Cu, Fe, Co, or Ni)[9,10] with trends found for the sulfidation of Mo after exposing X/Mo(110) surfaces to S_2 gas.[18−20] In general, a good correlation is observed between the changes in the two properties. This correlation suggests that a Ni-induced increase in the reactivity of Mo toward sulfur-containing molecules plays an important role in the high HDS activity of NiMoS catalysts. This is also implied by the theoretical results in section III.4 for the interaction of thiophene with Ni-promoted $MoS_2(10\bar{1}0)$-Mo clusters. In principle, the large HDS activity of NiMoS catalysts may result from the combination of three phenomena: (1) a Ni-induced rise in the coverage of atomic hydrogen can help to remove sulfur from the surface and keep a large number of unsaturated Mo atoms; (2) the existence of Ni centers on MoS_2(0002)-S terraces provides sites on which S-containing molecules can adsorb; and (3) the effects of Ni↔Mo and Ni↔S↔Mo interactions can make Mo more reactive for the desulfurization of organosulfur molecules. From the arguments at the beginning of this section, one can conclude that electronic interactions between the metals probably contribute to the performance of NiMoS catalysts, as proposed in previous studies.[9,11,12]

V. Conclusions

(1) The deposition of Ni and Zn atoms on a series of clusters (Mo_5S_{10}, Mo_6S_{12}, Mo_8S_{18}, Mo_9S_{18}, $Mo_{12}S_{24}$, and $Mo_{18}S_{36}$) that resemble the MoS_2(0002)-S and $MoS_2(10\bar{1}0)$-Mo surfaces produces a reduction in the stability (i.e., energy less negative) of the HOMOs of these systems. In all the cases examined, there was an admetal→MoS_2 charge transfer that increased the negative charge on sulfur and reduced the positive charge on molybdenum. The electronic perturbations induced by Ni were much larger than those induced by Zn.

(2) From a thermodynamic viewpoint, $MoS_2(10\bar{1}0)$-Mo clusters are more reactive toward atomic and molecular hydrogen than MoS_2(0002)-S clusters. The bonding interactions between H_2 and (0002)-S surfaces are weak, and promotion with Ni or Zn adatoms considerably improves the energetics for H_2 dissociation. On $MoS_2(10\bar{1}0)$-Mo, H_2 dissociation should be faster on bridge Mo sites than on a single Mo atom. Zn produces only minor changes in the energetics for H−H bond cleavage on this surface. In contrast, Ni largely raises the probability for H_2 dissociation by substantially increasing the stability of the transition state and products for this reaction.

(3) The adsorption energy of thiophene increases when going from MoS_2(0002)-S to $MoS_2(10\bar{1}0)$-Mo clusters. On the $(10\bar{1}0)$-Mo systems, the largest adsorption energy is found when the aromatic ring of thiophene is parallel to the surface and the molecule is simultaneously bonded to two adjacent Mo sites in η^1-S and η^5-S,C coordinations. This adsorption geometry leads to significant changes in the structure of the ring. Ni adatoms substantially enhance the strength of the C_4H_4S↔Mo bonding interactions, whereas Zn adatoms have negligible effects. Ni and Zn raise the chemical activity of MoS_2(0002)-S surfaces by providing active sites for the chemisorption of thiophene.

Acknowledgment. This work was carried out at Brookhaven National Laboratory and supported by the U.S. Department of Energy (DE-AC02-76CH00016), Office of Basic Energy Sciences.

References and Notes

(1) Weisser, O.; Landa, S. *Sulfide Catalysts: Their Properties and Applications*; Pergamon: Oxford, 1973.

(2) Speight, J. G. *The Chemistry and Technology of Petroleum*, 2nd ed.; McGraw-Hill: New York, 1991.

(3) Santiesteban, J. G. *Ph.D. Thesis*, Lehigh University, Bethelehem, PA, 1989.
(4) Tanaka, K. I.; Okuhari, T. *J. Catal.* **1982**, *78*, 155.
(5) Ho, T. C. *Catal. Rev.-Sci. Eng.* **1988**, *30*, 117.
(6) Startsev, A. N. *Catal. Rev.-Sci. Eng.* **1995**, *37*, 353.
(7) Chianelli, R. R.; Daage, M.; Ledoux, M. J. *Adv. Catal.* **1994**, *40*, 177.
(8) Dellmon, B. *Bull. Soc. Chim. Belg.* **1995**, *104*, 173.
(9) Harris, S.; Chianelli, R. R. *J. Catal.* **1986**, *98*, 17.
(10) Chianelli, R. R.; Pecoraro, T. A.; Halbert, T. R.; Pan, W.-H.; Stiefel, E. I. *J. Catal.* **1984**, *86*, 226.
(11) Zonnevylle, M.; Hoffmann, R.; Harris, S. *Surf. Sci.* **1988**, *199*, 320.
(12) Smit, T. S.; Johnson, K. H. *Catal. Lett.* **1994**, *28*, 361.
(13) Burdett, J. K.; Chung, J. T. *Surf. Sci.* **1990**, *236*, L353.
(14) Nørskov, J. K.; Clausen, B. S.; Topsøe, H. *Catal. Lett.* **1992,** *13*, 1.
(15) Bouwens, S. M. A. M.; van Veen, J. A. R.; Koningsberger, D.; de Beer, V. H. J.; Prins, R. *J. Phys. Chem.* **1991**, *95*, 123.
(16) (a) Vissers, J. P.; de Beer, V. H. J.; Prins, R. *J. Chem. Soc., Faraday Trans 1* **1987**, *83*, 2145. (b) Brito, J. L.; Barbosa, A. L.; Albornoz, A.; Severino, F.; Laine, J. *Catal. Lett.* **1994**, *26*, 329.
(17) Topsøe, H.; Clausen, B. S.; Topsøe, N.-Y.; Hyldtoft, J.; Nørskov, J. K. *Symposium on the Mechanism of HDS/HDN Reactions*; Division of Petroleum Chemistry, American Chemical Society, Chicago, IL, August 1993; American Chemical Society: Washington, DC, 1993.
(18) (a) Kuhn, M.; Rodriguez, J. A. *Surf. Sci.* **1996** *355*, 85. (b) Rodriguez, J. A. *Polyhedron* **1997**, *16*, 3177.
(19) Kuhn, M.; Rodriguez, J. A.; Hrbek, J. *Surf. Sci.* **1996**, *365*, 53.
(20) Rodriguez, J. A.; Li, S. Y.; Hrbek, J.; Huang, H. H.; Xu, G.-Q. *J. Phys. Chem.* **1996**, *100*, 14476.
(21) Rodriguez, J. A.; Li, S. Y.; Hrbek, J.; Huang, H. H.; Xu, G.-Q. *Surf. Sci.* **1997**, *370*, 85.
(22) Li, S. Y.; Rodriguez, J. A.; Hrbek, J.; Huang, H. H.; Xu, G.-Q. *Surf. Sci.* **1996**, *366*, 29.
(23) Whitten, J. L.; Yang, H. *Surf. Sci. Rep.* **1996**, *24*, 55.
(24) (a) van Santen, R. A.; Neurock, M. *Catal. Rev.—Sci. Eng.* **1995**, *37*, 557. (b) Ruette, F. Ed. *Quantum Chemistry Approaches to Chemisorption and Heterogeneous Catalysis*; Kluwer: Dordtrecht, 1992.
(25) (a) Ledoux, M. J.; Michaux, O.; Agostini, G. *J. Catal.* **1986**, *102*, 275. (b) Harris, S. *Chem. Phys.* **1982**, *67*, 229.
(26) Atencio, R.; Rincon, L.; Sanchez-Delgado, R.; Ruette, F. Submitted for publication.
(27) Neurock, M.; van Santen, R. *J. Am. Chem. Soc.* **1994**, *116*, 4427 and references therein.
(28) Kuhn, M.; Rodriguez, J. A. *Surf. Sci.* **1995**, *336*, 1.
(29) Rodriguez, J. A.; Kuhn, M. *J. Phys. Chem.* **1995**, *99*, 9567.
(30) Dupuis, M.; Chin, S.; Marquez, A. In *Relativistic and Electron Correlation Effects in Molecules and Clusters*; Malli, G. L., Ed.; NATO ASI Series; Plenum: New York, 1992.
(31) Anderson, W. P.; Cundari, T. R.; Zerner, M. C. *Int. J. Quantum Chem.* **1991**, *39*, 31.
(32) Wadt, W. R.; Hay, P. J. *J. Chem. Phys.* **1985**, *82*, 284.
(33) Hay, P. J.; Wadt, W. R. *J. Chem. Phys.* **1985**, *82*, 270.
(34) Rodriguez, J. A.; Kuhn, M. *Surf. Sci.* **1995**, *330*, L657.
(35) Rodriguez, J. A. *Surf. Sci.* **1996**, *345*, 347.
(36) Rodriguez, J. A.; Kuhn, M. *J. Phys. Chem.* **1996**, *100*, 381.
(37) Li, S. Y.; Rodriguez, J. A.; Hrbek, J.; Huang, H. H.; Xu, G.-Q. Submitted for publication.
(38) Zerner, M. C.; Loew, G. H.; Kirchner, R. F.; Mueller- Westerhoff, U. T. *J. Am. Chem. Soc.* **1980**, *102*, 589.
(39) Anderson, W. P.; Edwards, W. D.; Zerner, M. C. *Inorg. Chem.* **1986**, *25*, 2728.
(40) (a) Rodriguez, J. A. *Surf. Sci.* **1989**, *222*, 383. (b) Rodriguez, J. A.; Campbell, C. T. *Surf. Sci.* **1988**, *206*, 426. (c) Rodriguez, J. A. *Surf. Sci.* **1990**, *226*, 101. (d) Rodriguez, J. A. *Surf. Sci.* **1992**, *278*, 326. (e) Rodriguez, J. A.; Campbell, C. T. *J. Phys. Chem.* **1987**, *91*, 2161; 6648.
(41) (a) Wells, A. F. *Structural Inorganic Chemistry*; Oxford Univerity Press: New York, 1987. (b) Dickinson, R. G.; Pauling, L. *J. Am. Chem. Soc.* **1923**, *45*, 1466.
(42) Mitchell, K. A. R. *Surf. Sci.* **1985**, *149*, 93.
(43) *Comprehensive Coordination Chemistry*; Wilkinson, G., Gillard, R. D., McCleverty, J. A., Ed.; Pergamon Press: New York, 1987; Chapters 16, 50, and 56.
(44) Kittel, C. *Introduction to Solid State Physics*, 6th ed.; Wiley: New York, 1986; p 76.
(45) Anderson, A. B.; Al-Saigh, Z. Y.; Hall, W. K. *J. Phys. Chem.* **1988**, *92*, 803.
(46) Rong, C.; Qin, X. *J. Mol. Catal.* **1991**, *64*, 321.
(47) Papageorgopoulos, C.; Kamaratos, M. *Surf. Sci.* **1985**, *164*, 353.
(48) Mulliken, R. S. *J. Chem. Phys.* **1955**, *23*, 1841.
(49) (a) In the INDO/S calculations, the charges were estimated by a Mulliken population analysis[48] using the overlap matrix and the deorthogonalized INDO eigenvector matrix.[49b] (b) Shillady, D. D.; Billingsley, F. P.; Bloor, J. E. *Theor. Chim. Acta* **1971**, *21*, 1.
(50) Szabo, A.; Ostlund, N. S. *Modern Quantum Chemistry*; McGraw-Hill: New York, 1989.
(51) The Mulliken population analysis depends strongly on the type of basis set used to describe the atomic orbitals of the elements.[50] This is a serious limitation that makes meaningless a quantitative comparison of the charges coming from the ab initio, INDO/S, ASED, and DV-Xα calculations.
(52) Baker, R. T. K.; Chludzinski, J. J.; Sherwood, R. D. *J. Mater. Sci.* **1987**, *22*, 3831.
(53) (a) Roberts, J. T.; Friend, C. M. *Surf. Sci.* **1987**, *186*, 201. (b) Zaera, F.; Kollin, E. B.; Gland, J. L. *Surf. Sci.* **1987**, *184*, 75. (c) Fulmer, J. P.; Zaera, F.; Tysoe, W. T. *J. Phys. Chem.* **1988**, *92*, 4147.
(54) (a) Angelici, R. J. *Acc. Chem. Res.* **1988**, *21*, 387. (b) Riaz, U.; Curnow, O. J.; Curtis, M. D. *J. Am. Chem. Soc.* **1994**, *116*, 4357. (c) Sanchez-Delgado, R. A. *J. Mol. Catal.* **1994**, *86*, 287. (d) Arce, A. J.; De Santis, Y.; Karam, A.; Deeming, A. J. *Angew. Chem. Int. Ed. Engl.* **1994**, *33*, 1381.
(55) Harshbarger, W. R.; Bauer, S. H. *Acta Crystallogr. B* **1970**, *26*, 1010.
(56) Salmeron, M.; Somorjai, G. A.; Wold, A.; Chianelli, R.; Liang, K. S. *Chem. Phys. Lett.* **1982**, *90*, 105.
(57) Hout, R. F.; Pietro, W. J.; Hehre, W. J. *A Pictorial Approach to Molecular Structure and Reactivity*; Wiley: New York, 1984; pp 273−275.
(58) Rodriguez, J. A. *Surf. Sci.* **1990**, *234*, 421.
(59) Derrick, P. J.; Åsbrink, L.; Edqvist, O.; Jonsson, B. O.; Lindholm, E. *Int. J. Mass Spectrom. Ion Phys.* **1971**, *6*, 177.
(60) The adsorption geometries of thiophene in the INDO/S studies were set equal to those found in the ab initio SCF calculations for the $C_4H_4S/NiMo_6S_{12}$ system.
(61) Diemann, E.; Weber, T.; Muller, A. *J. Catal.* **1994**, *148*, 288.